Reprinted from the Journal of the Institution of Electronics and Telecommunication Engineers, Vol. 33, No. 1, 1987, pp 22-29

13

Accurate Estimation of ILS Glideslope in the Presence of Terrain Irregularities

M M POULOSE, FIETE, P R MAHAPATRA AND N BALAKRISHNAN

Department of Aerospace Engineering, Indian Institute of Science, Bangalore 560 012 India

The primary emphasis of this paper is to evolve a general analytical method for the accurate prediction of glideslope aberrations in aircraft instrument landing systems (ILS) in the presence of known terrain features. Methods of mathematical modelling for electric fields in the presence of arbitrary reflecting boundaries are critically analysed, and graded according to their applicability to the evaluation of glideslopes in ILS. Using a multiple plate model of the terrain, a series of computer programs is developed to compute glideslopes using the Uniform Theory of Diffraction (UTD) and, for the first time, Uniform Asymptotic Theory (UAT). The programs are most general in terms of handling combinations of rays of various orders. An innovative algorithm for direct determination of the point of diffraction at an edge is incorporated.

Results have been generated for several airports in India and those pertaining to Madras airport are presented in this paper. The results, computed for conditions corresponding to actual flight tests, are in excellent agreement with flight measured data. This establishes the model developed here as a practical and economical method of accurately predicting site behaviour of proposed ILS glideslope equipment.

Indexing terms : ILS, UTD, UAT, GTD

THE INSTRUMENT LANDING SYSTEM (ILS) provides the pilot of an aircraft with steering information to make an accurate and controlled runway approach and landing even under adverse weather conditions [1]. This is accomplished by the provision of azimuth guidance, elevation guidance and distance-from-threshold information.

The main constituents of the ILS are the localiser, glidepath and marker beacons [1], [2]. The localiser, operating in the 108-112 MHz band, provides azimuth guidance information through the differential depth of modulation (ddm) of two signals at 90 and 150 Hz. The ddm is zero on a vertical plane through the centre line of the runway and varies linearly over the course sector. The elevation guidance is provided by the glideslope equipment in the 328-336 MHz band, also operating on the ddm principle with 90 and 150 Hz tones.

Simultaneous nulling of the ddm from localiser and glidepath equipment is expected to define a straight line descent path, at a desired elevation angle, lying in the vertical plane passing through the runway centre line. However, an aircraft on or near the glidepath receives not only the direct signals from the antenna system but also signals reflected from the intervening terrain. The effect of

Paper No 6B; copyright © IETE, 1987
Manuscript received 1986 February 19; revised 1986 July 28.

terrain must be taken into account in determining the course provided by the glidepath equipment.

Most widely used antenna designs make use of reflection characteristics of an ideal ground to establish a proper glidepth [3]. The design of arrays is based on image theory in which the ground plane is idealised as being infinite and perfectly conducting. Since the elevation angles involved are small and wavelengths fairly large, wide stretches of plane ground must be available in front of the antenna to obtain a reasonable approximation to the ideal image patterns.

The presence of unevenness, reflectivity fluctuations or other irregularities in the ground around the glideslope antenna causes kinks and bends in the electronically defined glideslope. An aircraft trying to follow such a course is subjected to unnecessary maneuvers and, in extreme cases where the undulations come close to the ground or other obstructions, the result may be fatal. Glideslope aberrations have been implicated in serious aircraft accidents in the past. It is therefore clearly desirable to have an estimate of the quality of glideslope that may be obtained at specific ILS locations at the planning stage itself. Such estimates can be obtained experimentally through actual in-flight measurements with temporary installations. However, such installations as well as flight calibration operations are very expensive. More importantly, this procedure would only give glideslope data for the existing terrain and cannot provide insight into remedial measures such as terrain development, system re-configuration etc.

These difficulties would be largely overcome by accurate mathematical modelling which would be far less expensive, and provide results for any assumed terrain and system configuration. Considerable effort has therefore been made in the last decade to mathematically model the terrain, and various techniques based on Physical Optics (PO) [4], [5] and Geometrical Theory of Diffraction (GTD) [6] have been put forward.

The PO technique is based on assumed ground currents which are integrated to obtain the scattered field from the reflecting terrain. In applying this method, the simplifying assumption is usually made that ground currents in one area have no effect on the neighbouring areas. Such an assumption is necessary to determine the fields within reasonable computation time, but it implies that the electric fields radiated by the ground pass through any subsequent obstructions as if they do not exist.

An attempt has been made in the Physical Theory of Diffraction (PTD) to include the mutual interactions by considering an edge current [7]. However, PTD is rather unattractive because of the complicated formulation and large computer resources required [8].

A model developed by Godfrey *et al* [9] is based on the half-plane diffraction solution of Senior [10], Woods [11] and Bromwich [12]. This is useful in modelling glideslope sites with finite flat reflecting surface in front of the antenna which then drops off sharply to terrain which is either shadowed from the antennas or is so rough that it does not reflect coherently. Redlich's model [13], [14] uses diffraction theory which allows for the presence of an infinite plane located below a half plane. However this model can handle only limited terrain configurations.

The excessive computational requirements of PO methods have led to the search for ray-based theories or those based on Geometric Optics (GO) [15]. The simplest application of GO to the study of terrain effects considers only the direct rays and the rays reflected from the terrain. While it can account for terrain slopes and reflectivity aspects, it results in discontinuities in the computed field in the presence of terrain drop-offs.

The Geometrical Theory of Diffraction (GTD) developed by J.B. Keller [16], [17] overcomes the problem associated with the GO methods by considering the diffracted rays in addition to direct and reflected rays. But in this formulation, the fields become infinite at the reflection and shadow boundaries, whereas far from these boundaries, the field prediction is accurate.

This drawback has been overcome by the Uniform Theory of Diffraction (UTD) and Uniform Asymptotic Theory (UAT). In the UTD [18], [19] diffraction co-efficient is modified by introducing cotangent and Fresnel functions. In the UAT of Ahluwalia *et al* [20]—[22], the diffraction term is left unaltered and the geometric field is modified in such a way that it results in a finite value of the total field at the reflection and shadow boundaries.

The basic theories behind the methods enumerated above can be used to determine essentially the fields generated by the presence of individual terrain elements. Though several glidepath antenna types exist [23], [24] with different influence of the surroundings on the system performance in each case, the siting or location of the antenna system is critical in all the cases.

This paper describes an efficient computer terrain model to evaluate the terrain effects on ILS glideslope. Both UTD and UAT techniques have been employed to evaluate the fields in the presence of the terrain. The model is applied to several actual airports in India and the computed results are compared with aircraft measured data. Consistently good agreement is obtained and a sample case is presented here.

THEORY

The ILS image glideslope antenna system typically consists of two or three elements, each excited depending on the type of the system employed. Table 1 provides details of antenna location and relative excitations.

The resultant field at an observation point may be

TABLE 1 Nominal relative antenna currents and their locations in image glidepath system

Antenna element No.	Null Ref Ht	Null Ref CSB	Null Ref SBO	Sideband Ref Ht	Sideband Ref CSB	Sideband Ref SBO	Capture Effect Ht	Capture Effect CSB	Capture Effect SBO
1	h	1	0	0.5h	1	—1	h	1	—0.5
2	2h	0	1	1.5h	0	1	2h	—0.5	1
3	—	—	—	—	—	—	3h	0	—0.5

Notes : (1) CSB = Carrier-plus-sideband, SBO = Sideband only
(2) $h = \lambda/(4\sin\theta)$ where θ is the glide angle and λ wavelength

obtained by the superposition of fields due to individual antenna elements. The contribution of the electromagnetic theory to the current problem arises through the method of computing the field at the observation point due to a single antenna element in the presence of a reflecting terrain. This section outlines the adaptation of the ray theoretic approach to the field computation assuming the antenna element to be a point source.

Field computation

Total field at an observation point can be written as

$$\mathbf{E}^t_{s,h} = \mathbf{E}^s + \mathbf{E}^d = \mathbf{E}^{di} + \mathbf{E}^r_{s,h} + \mathbf{E}^d_{s,h} \qquad (1)$$

where $\mathbf{E}^{di}$, $\mathbf{E}^r$ and $\mathbf{E}^d$ are the direct, reflected and diffracted fields respectively. Substituting for these in equation (1) [16],

$$\mathbf{E}^t_{s,h} = E_0 \left[\frac{\exp(-jks_0)}{s_0} \mp \frac{\exp(-jks'')}{s''} + \frac{\exp(-jks')}{s'} \mathbf{D}_{s,h} \exp(-jks) A_d \right] \qquad (2)$$

where $A_d = [s'/s(s+s')]^{1/2}$ (2a)

and

$$\mathbf{D}_{s,h} = \frac{e^{-j\pi/4} \sin\pi/n}{n\sqrt{2\pi k} \sin\beta_0} \left[\frac{1}{\cos\pi/n - \cos\beta^-/n} \mp \frac{1}{\cos\pi/n - \cos\beta^+/n} \right] \qquad (3)$$

The various parameters referred to in above equations are shown in Fig 1.

The main drawback of the above GTD approach is the singularity in the diffraction co-efficient and therefore in the field at the reflection boundary ($\phi+\phi' = \pi$) and the shadow boundary ($\phi-\phi' = \pi$).

The uniform theories obviate this drawback.

The approach of the UTD technique is to modify Keller's diffraction co-efficient in (3). The UTD diffraction co-efficient, which can be applied to any wedge configuration, is given by [18]

$$\mathbf{D}_{s,h}(\phi,\phi',\beta) = \frac{-\exp(-j\pi/4)}{2n(2\pi k)^{1/2} \sin\beta_0} \times \left[\cot\left(\frac{\pi+(\phi-\phi')}{2n}\right) F[k\,La^+(\phi-\phi')] + \cot\left(\frac{\pi-(\phi-\phi')}{2n}\right) F[k\,La^-(\phi-\phi')] \mp \left\{ \cot\left(\frac{\pi+(\phi+\phi')}{2n}\right) F[k\,La^+_+(\phi+\phi')] + \cot\left(\frac{\pi-(\phi+\phi')}{2n}\right) F[k\,La^-_+(\phi+\phi')] \right\} \right] \qquad (4)$$

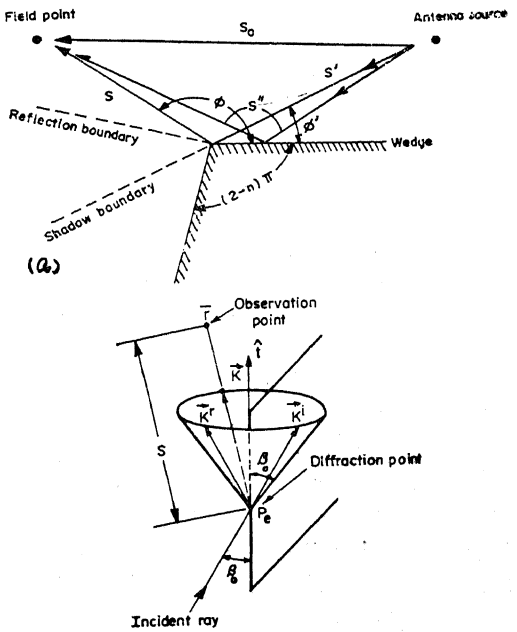

Fig 1 (a) Diffraction and reflection at a wedge, (b) Cone of diffracted rays

where

$$F(x) = 2j\,|\sqrt{x}\,|\exp(jx) \int_{|\sqrt{x}|}^{\infty} \exp(-j\tau^2)d\tau \qquad (4a)$$

$$a^{\pm}_{\pm} = 2\cos^2\left(\frac{2n\pi N^{\pm}_{\pm} - \beta^{\pm}}{2}\right) \qquad (4b)$$

$N^{\pm}_{\pm}$ = the integers which most nearly satisfy the following equations,

$$2\pi n N^{+}_{\pm} - \beta^{\pm} = \pi \qquad (4c)$$

$$2\pi n N^{-}_{\pm} - \beta^{\pm} = -\pi \qquad (4d)$$

and

$$\beta^{\pm} = \phi \pm \phi' \tag{4e}$$

The distance parameter for spherical wave incidence is given by

$$L = \frac{ss'}{s+s'} \sin^2\beta_0 \tag{4f}$$

At reflection and shadow boundaries, one of the cotangent functions in [4] becomes singular. But the product of this cotangent function and the Fresnel function is still finite.

When the observation point moves away from the reflection and shadow boundaries, (4) is reduced to (3). Under this situation, the observation point is said to be outside the transition regions.

The UAT introduced by Ahluwalia *et al* [20] has been further developed by Lee and Deschamps [21, 22]. Both UTD and UAT are based on different ansatz and yield different expressions for high frequency asymptotic solution of the edge diffraction problem that are uniformly valid in the entire space including transition regions around the shadow boundaries.

In the UAT, the total field $\mathbf{E}^t$ is given by

$$\mathbf{E}^t_{s',h} = \mathbf{E}^G + \mathbf{E}^d \tag{5}$$

When the UAT solution is compared with the GTD solution in equation (1), it is noticed that the diffracted field $\mathbf{E}^d$ is unchanged while the geometric optics field $\mathbf{E}^g$ is modified to take care of the singularities at the shadow and reflection regions.

The modified geometric optic field $\mathbf{E}^G$ in (5) is given by

$$\mathbf{E}^G = [\mathbf{F}(\xi^i) - \hat{\mathbf{F}}(\xi^i)]\,\mathbf{E}^i + [F(\xi^r) - \hat{F}(\xi^r)]\mathbf{E}^r \tag{6}$$

where $$F(x) = (\pi)^{-1/2} \exp[-j\pi/4] \int_x^{\infty} \exp(jt^2)dt \tag{7a}$$

$$\hat{F}(x) = [2x(\pi)^{1/2}]^{-1} \exp[j\{x^2+(\pi/4)\}] \tag{7b}$$

$$\xi^i = \mp (k)^{1/2} \mid (s'+s-s_0)^{1/2} \mid \tag{7c}$$

and $$\xi^r = \mp (k)^{1/2} \mid (s'+s-s'')^{1/2} \mid \tag{7d}$$

where the positive and negative signs correspond to the shadow and lit regions respectively.

It can easily be seen that when the observation point is away from the shadow boundaries, the detour parameters ξ^i and ξ^r are large and the expression for the modified geometric optics field reduces to the geometric optics field and the UAT recovers the GTD solution.

As is obvious, the main contribution of UAT is to modify the GTD near the shadow and reflection boundaries where ξ^i and ξ^r are small. Exactly on these boundaries both $\mathbf{E}^G$ and $\mathbf{E}^d$ become infinite in such a manner that their singular parts cancel each other and hence $\mathbf{E}^t$ remains finite and continuous across the boundaries.

TERRAIN MODELLING

The ILS glideslope antenna system is mounted on a single mast located with respect to a runway as shown in Fig 2a. Aircraft operations may be assumed to remain confined to a vertical plane passing through the runway centre line. In such a case significant perturbation effects are produced by the terrain along the vertical plane passing through the antenna and the aircraft. This section of the terrain is called the profile line and is shown in Fig 2*a*. Far away from the profile line, only large features contribute significant scattered energy and are not considered in this work. Focussing attention only on the profile line permits a 2-D treatment of the terrain.

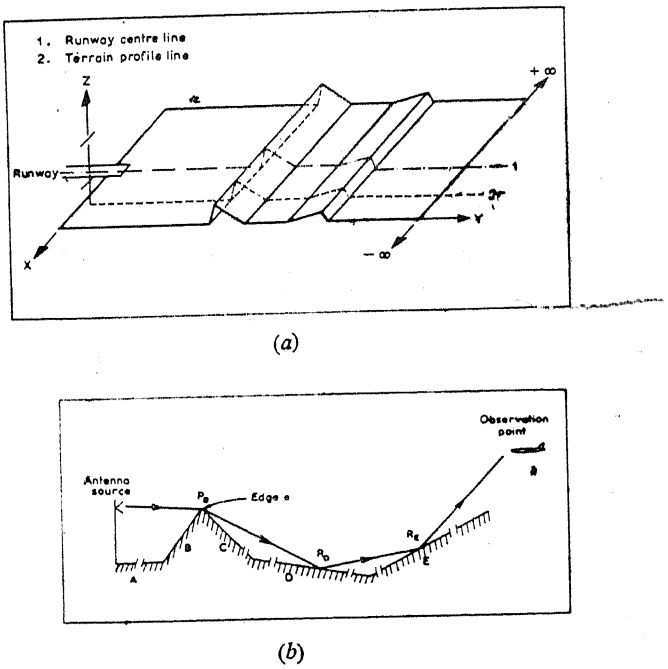

(*a*)

(*b*)

Fig 2 (*a*) Two dimensional terrain model,
(*b*) Diffracted-reflected-reflected ray, diffracted from edge *e* to plate *D*, reflected from plate D to E and reflected from plate *E* to observation point

For simplicity, the profile line is described in terms of a relatively small number of straight line segments and the terrain height is assumed invariant in a direction prependicular to the runway. This permits a wedge description of the terrain for glideslope modelling purposes as shown in Fig 2*a*.

Smooth wedges with perfect conductivity are considered here. At grazing incidence angles, the perfect conduction assumption is very close to reality. The effect of normal levels of surface roughness has been shown to be negligible in ILS applications [25]. The effect of roughness is a reduction of the coherent scattered signals and an increase in the incoherent signals. The terrain of the airport is usually smooth enough in relation to glidepath signal wavelength (about 1 m) that the coherent signal will dominate. For small roughness compared to wavelength, it has been shown that [26], the effect on the scattered

signal can be substituted by an equivalent surface impedance. Then the problem may be treated by using an appropriate theory such as that developed by James [27] for an impedance wedge. Using the above terrain model, and the formulation outlined in the previous section, concrete results have been generated and reported in this paper, and compared with actual flight measurements.

RAY TYPES, THEIR EXISTENCE AND ORDER EFFECTS

Determination of ray types is a major step in the field evaluation using ray-theoretic approach in the case of a multiwedge terrain model. The earlier investigators have made some simplifying assumptions with regard to the ray groups; in this study algorithms have been developed which exhaustively test for all rays of any order and combination. This means that the primary three ray types *viz.* Direct (D), Reflected (R) and Diffracted (D_f) rays from each plate/edge in the terrain model can be combined in any order upto any level (*eg* D, R, D_f, RD_f, $D_f RR$ etc) and the computer model would automatically check for the existence of the particular combination for the given antenna and observation location. For each ray that is found to exist, the model would proceed to compute the vector field contribution at the observer point. To provide a brief explanation of the algorithms developed, consider a diffracted-reflected-reflected (D_fRR) ray shown in Fig 2*b*. This is a ray diffracted once from an edge and reflected from two other plates. The diffracting edge here is obviously not a part of the reflecting plates.

The ray existence algorithm starts with a test for the existence of the diffraction and reflection points. This is achieved by imaging the observer location with respect to plate E (Fig 2*b*) and using this image location, a secondary image location with respect to plate D is obtained. The diffraction point P_e satisfies the law of edge diffraction (Fermat's principle). Instead of an iterative algorithm used in the past for the determination of the diffraction point, an efficient non-iterative algorithm has been developed in this study which reduces the computer time substantially.

After the existence test, the program proceeds further to ensure that the rays from the antenna (Fig 3) to P_e, P_e to R_D, R_D to R_E and R_E to the observation point are not blocked by other obstructions. If the above path is not blocked, then the D_fRR ray is accepted as valid and its contribution calculated and added to the previous contributions.

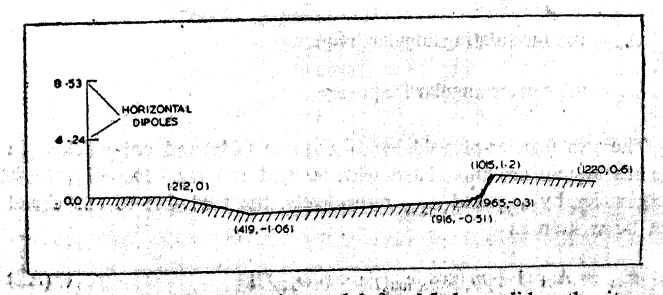

Fig 3 Approximate terrain model for Madras glidepath site

The process is repeated until all combinations of edge and plates have been examined. The total diffracted-reflected-reflected field is given by

$$\mathbf{E}^{DRR} = \sum_{e}^{e_t} \sum_{D}^{N} \sum_{E}^{N} \mathbf{E}^{DRR}_{E,D,E} \qquad (8)$$

where e = the edge index

e_t = the total number of edges

D,E = plate indexes

N = Number of modelling plates

$\mathbf{E}^{DRR}_{E,D,E}$ = the D_fRR field

Similar algorithms have been developed for the determination and evaluation of various other ray combinations upto order three. Actual computation shows that a CPU time of less than 5 minutes in a Dec-10 computer is required when 12 modelling plates are considered, with all the ray combinations, for an 80-point simulation along the aircraft flight path.

APPLICATION TO A REAL SITE

The treatment outlined in the earlier sections has been applied to several actual airport sites in India with encouraging results. For illustration here, the runway 07 at Madras Airport is considered. The terrain has no significant lateral variations (*i e* less than one foot). The glidepath antenna is located at 1000 feet from the 07 end, offset by 450 feet. The operating frequency is 335 MHz. Six conducting plates are used to model the terrain as shown in Fig 3.

As per ICAO standards [28], usually the flight validation process includes a level run and a low-level approach for measuring the vertical and structure characteristics of the glideslope. The measuring aircraft is instrumented to record the DDM values at various observation points resulting from the composite antenna system. No direct measurement of individual antenna element patterns is possible. To be able to compare on a standard basis, therefore, the computed field strengths due to various antenna elements are reduced to equivalent DDM values using the theory in Appendix A and the values are compared with measured DDM values. Figure 4 is a plot of the

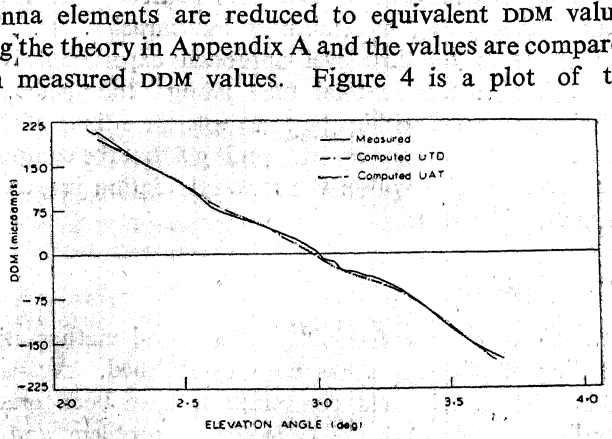

Fig 4 Curve showing DDM Vs elevation angle for a 1000-foot level run

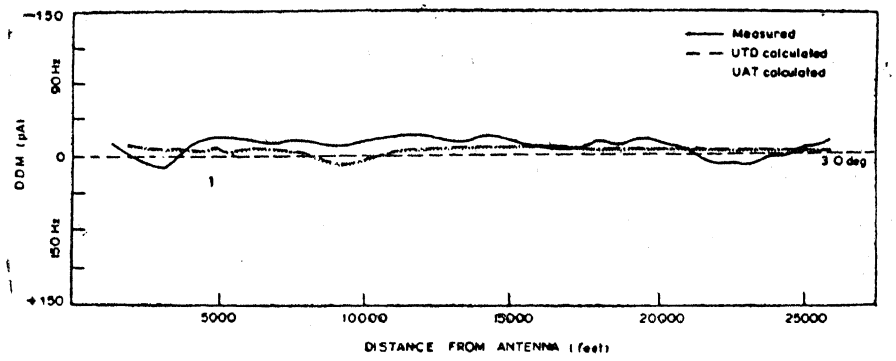

Fig 5 Curve showing DDM vs distance for low-level approach

measured and computed DDM as a function of the elevation angle for a level run at 1000 ft altitude. Glideslope parametres derived from these runs are shown in Table 2.

TABLE 2 Measured and computed parameters for a 1000-foot level run at Madras 07 runway

Parameter	Measured	Calculated	
		UAT	UTD
Path angle (deg)	3	2.98	2.98
Lower sector width (deg)	0.35	0.33	0.323
Upper sector width (deg)	0.37	0.36	0.353
CPU time (sec)		92.6	69.34

The difference between the measured and computed path angle is only 0.02 degrees. Against a total measured course width of 0.72 degrees, the computed value is 0.69 which also shows good agreement. The UAT technique requires about 33% more CPU time as compared to UTD.

Figure 5 shows the computed and measured DDM versus distance for a low-level approach. Here since the aircraft always remains in a zone of low DDM, the predominant component of error is random, caused by navigation uncertainties, gusts, measurement inaccuracies, etc. The crucial test in the low-level approach experiment is to check whether the residual DDM along the geometric glideslope remains within the ICAO tolerance limit of ± 30 microamps [29]. It is noticed from Fig 5 that the computed DDM range remains within the ICAO stipulation just as the measured value does.

CONCLUSION

In this paper, the feasibility of a sound mathematical nodelling of glideslopes has been established. Available nethods of electric field computation have been graded ccording to their applicability to the ILS problem, and the ıore admissible methods have been critically analysed. Based on these methods and a plate-modelled terrain along with a DDM computation algorithm, a complete chain for evaluating the glideslope aberrations has been established. A computer program to implement this procedure has been written, exhaustively covering all possible rays, and the results corresponding to a representative actual terrain profile is presented. The program incorporates several innovative features such as the most general ray-order formulation and a non-iterative technique for locating the diffraction point on an edge. The experience gained from this study shows that sophisticated mathematical modelling can yield results very close to true or measured data on glideslopes. Thus, modelling can be a low cost, fast and versatile method of site evaluation for ILS installation.

ACKNOWLEDGEMENT

The authors wish to acknowledge the contributions of Shri MS Krishnan, Director of Communication, Madras Airport, and the encouragement received from Air Marshal CKS Raje, Chairman, National Airports Authority of India in carrying out this study.

APPENDIX A

DDM Computation

The far field in front of the antenna may be represented by

$$\mathbf{E} = \mathbf{A}\,[1+m\cos\omega_m t]\exp i\omega_c t \qquad \text{(A1)}$$

where $\mathbf{A}$ = field vector whose amplitude is inversely proportional to the distance from the antenna and phase directly proportional to distance.

m= modulation index

ω_m= the modulating angular frequency

ω_c= the carrier angular frequency

The CSB (carrier-plus-sideband) and SBO (sideband only) fields in the ILS system are modulated with 90 and 150 Hz. Denoting these frequencies by ω_{90} and ω_{150} respectively, the field due to CSB signal can be written as

$$\mathbf{E}_{cs} = \mathbf{A}_{cs}\,[1+m\,(\cos\omega_{90}t+\cos\omega_{150}t)] \qquad \text{(A2)}$$

where the subscript *cs* refers to the CSB signal. Similarly, the field due to SBO can be written as

$$E_{sb} = A_{sb}\, m\, [\cos \omega_{90}t - \cos \omega_{150}t] \quad \text{(A3)}$$

where the subscript *sb* refers to SBO signal.

The total complex field envelope at the observation point (aircraft) is the sum of the CSB and SBO fields.

The detector at the aircraft receiver outputs a signal proportional to the amplitude of the total field envelope. The normalized detector output E_{od} can be represented as

$$E_{od} = |\, (E_{cs}+E_{sb})/A_{cs} \,| \quad \text{(A4)}$$

Substituting for E_{cs} and E_{sb} from equations (A2) and (A3) and simplifying, (A4) reduces to

$$E_{od} = [(1+E_1)^2+E_2^2]^{1/2}$$
$$= [1+2E_1+E_1^2+E_2^2]^{1/2} \quad \text{(A5)}$$

where $E_1 = m\,[1+\text{Re}\,(A_{sb}/A_{cs})]\cos \omega_{90}t$
$$+ m\,[1-\text{Re}\,(A_{sb}/A_{cs})]\cos \omega_{150}t \quad \text{(A6)}$$

and $E_2 = \text{Im}\,(A_{sb}/A_{cs})\, m \cos(\omega_{90}t - \omega_{150}t)$ (A7)

Expanding (A5) as a power series,

$$E_{od} = 1+[(2E_1+E_1^2+E_2^2)/2]-[(2E_1+E_1^2+E_2^2)/8]^2$$
$$+\text{higher order terms.} \quad \text{(A8)}$$

E_1 contains undistorted 90 and 150 Hz signals. E_1^2 and E_2^2 contain harmonics of 90 and 150 Hz signals and their sums and differences. The third and higher order terms contain harmonics and cross product frequencies including some additional small amplitude 90 and 150 Hz signals. The detector output is passed through 90 and 150 Hz filters.

Neglecting the contributions from the third and higher order terms, the outputs from these filters can be considered to come from E_1 in the second term of equation (A8). Therefore, the outputs from 90 and 150 Hz filters can be written as

$$E_{90} = m\,[1+\text{Re}\,(A_{sb}/A_{cs})] \quad \text{(A9)}$$

and

$$E_{150} = m\,[1-\text{Re}\,(A_{sb}/A_{cs})] \quad \text{(A10)}$$

The DDM signal is obtained by taking the difference between E_{90} and E_{150} signals obtained above. DDM is therefore given by

$$\text{DDM} = E_{90}-E_{150} = 2m\ \text{Re}\,(A_{sb}/A_{cs}) \quad \text{(A11)}$$

Glidepath systems are normalized so that at ± 0.35 degrees relative to the desired path angle, the aircraft DDM indicator reads ± 75 microamperes. Thus, the normalized DDM can be represented as

$$\text{DDM}_{\mu A} = 150\ \frac{\rho}{|\,\rho\,|_{0.35}+|\,\rho\,|_{-0.35}} \quad \text{(A12)}$$

where $\rho = \text{Re}\,(A_{sb}/A_{cs})$ (A13*a*)

and $|\,\rho\,|_{\pm 0.35} =$ value of ρ at $\Delta\theta = \pm 0.35°$ (A13*b*)

The value of the field contributions A_{sb} and A_{cs} due to the SBO and CSB antenna elements can be computed using the field computation methods.

In ILS hand book and operating literature, for instinctive understanding, the formulae (A11) and (A12) are represented respectively as

$$\text{DDM} = 2\ \text{m Re}\,(\text{SBO/CSB}) \quad \text{(A14)}$$

$$\text{DDM}_{\mu A} = 75\,\frac{\text{Re(SBO/CSB)}}{\frac{1}{2}[|\text{Re(SBO/CSB)}|_{\Delta\theta=0.35°}+|\text{Re(SBO/CSB)}|_{\Delta\theta=-0.35°}]} \quad \text{(A15)}$$

REFERENCES

1 Plessey Radar, Addletone, England: Technical Manual on ILS, vol TP 3140, Sep 1972

2 Federal Aviation Administration, Installation Instruction for ILS, DOT/FAA Handbook No. 6750.6A, 1969

3 P C Sandretto, Aviation Engineering, New York International Telephone and Telegraph Corporation, 1958, pp 656–672.

4 S Ramakrishna and M Sachidananda, Calculating the Effect of Uneven Terrain on Glidepath Signals, *IEEE Trans*, vol AES-10, pp 380–384, May 1974

5 S Morin *et al*, ILS Glideslope Performance Prediction, Report FAA-RD-74-157. B, Transportation System Centre, Cambridge, Massachussets, Sep 1974

6 R Luebbers *et al*, GTD Terrain Reflection Model Applied to ILS Glideslope, *IEEE Trans*, vol AES-8, pp 11–19, Jan 1982

7 R A Ufimstev, *Method of Edge Waves in Physical Theory of Diffraction*, US Airforce Foreign Technology Division, Wright Patterson AFB, Dayton, Ohio, USA, 1962

8 G L James, Geometrical Theory of Diffraction for Electromagnetic Waves, Peter Peregrinus Ltd, London, 1980

9 J T Godfrey *et al*, Terrain Modelling Using the Half Plane Geometry with Applications to ILS Glideslope, *IEEE Trans*, vol AP-24, pp 370–378, May 1976

10 T B A Senior, The Diffraction of a Dipole Field by a Perfectly Conducting Half Plane, *Quarterly Journal of Mechanics and Applied Mathematics*, vol VI, Pt 1, p 101, 1953

11 B D Woods, The Diffraction of a Dipole Field by a Half Plane, *ibid*, vol X, Pt 1, p 90, 1957

12 T J I A Bromwich, *Proc London Math Soc*, vol 14, p 450, 1915

13 R W Redlich, Image Radiation from a Finite Ground Plane in Two Dimensions, *IEEE Trans*, vol AP-16, pp 334–337, May 1968

14 R W Redlich, Computed Performance of Glideslope Arrays on Sites with Limited Ground Plane, *IEEE Trans*, vol AES-7, pp 854–862, Sep 1971

15 M Born & E Wolf, Principles of Optics, Pergamon Press, New York, p 108, 1959

16 J B Keller, Geometrical Theory of Diffraction, *Journal of the Optical Society of America*, vol 52, pp 116–130, 1962

17 J B Keller *et al*, The Geometrical Theory of Diffraction, Proceedings of the Symposium on Microwave Optics, Eaton Electronic Research Lab, McGill University, Montreal, Canada, Jun 1953

18 Kouyoumjian and Pathak, A Uniform Geometrical Theory of Diffraction for an Edge on a Perfectly Conducting Surface, *Proc IEEE*, vol 62, pp 1448–1461, Nov 1964

19 R Tiberio & Kouyoumjian, A Uniform GTD Analysis of Diffraction by Thick Edges and Strips Illuminated at Grazing Incidence, International Symposium Digest, Antenna and Propagation, Uni of Maryland, May 1978

20 Ahluwalia *et al*, Uniform Asymptotic Theory of Diffraction by a Plane Screen, *SIAM Journal of Applied Mathematics*, vol 16, pp 783–807, Jul 1968

21 S W Lee & G A Deschamps, A Uniform Asymptotic Theory of Electromagnetic Diffraction by a Curved Wedge, *IEEE Trans*, vol AP-24, pp 25–34, 1976

22 G A Deschamps *et al*, Three Dimensional Half Plane Diffraction, Exact Solution and Testing of Uniform Theories, *IEEE Trans*, vol AP-32, pp 264–271, Mar 1984

23 R H MacFarland, Application of Endfire Arrays at Contemporary Glideslope Problem Sites, *IEEE Trans*, vol AES-7, pp 261–269, Mar 1981

24 R H MacFarland, Flush Mounted Glidepath System, *IRE Trans*, vol ANE-9, pp 211–215, Dec 1962

25 T Brein, *Multipath Analysis of ILS Glidepath*, ELAB, Norway, N-7034, 1979

26 T B A Senior, Impedance Boundary Conditions for Statistically Rough Surfaces, *App Sci Res*, Sec B, 1960, pp 437–468

27 G L James, Uniform Diffraction Coefficient for an Impedance Wedge, *Electronic Letters*, pp 403–404, 1977

28 Manual on Testing of Radio Navigational Aids, vol II, International Civil Aviation Organisation (ICAO), Montreal, Canada, 1973

29 Aeronautical Telecommunications Anex 10, International Civil Aviation Organisation, Montreal, Canada, p 93, 1968

* * * *